Blue Light-Operated CRISPR/Cas13b-Mediated mRNA Knockdown (Lockdown)

Tim Blomeier, Patrick Fischbach, Leonie-Alexa Koch, Jennifer Andres, Miguel Miñambres, Hannes Michael Beyer, and Matias Daniel Zurbriggen*

The introduction of optogenetics into cell biology has furnished systems to control gene expression at the transcriptional and protein stability level, with a high degree of spatial, temporal, and dynamic light-regulation capabilities. Strategies to downregulate RNA currently rely on RNA interference and CRISPR/Cas-related methods. However, these approaches lack the key characteristics and advantages provided by optical control. "Lockdown" introduces optical control of RNA levels utilizing a blue light-dependent switch to induce expression of CRISPR/Cas13b, which mediates sequence-specific mRNA knockdown. Combining Lockdown with optogenetic tools to repress gene-expression and induce protein destabilization with blue light yields efficient triple-controlled downregulation of target proteins. Implementing Lockdown to degrade endogenous mRNA levels of the cyclin-dependent kinase 1 (hCdk1) leads to blue light-induced G2/M cell cycle arrest and inhibition of cell growth in mammalian cells.

The integration of optogenetic switches into a broad range of molecular tools has recently revolutionized biological studies by opening the possibility to control cellular processes with unmatched spatiotemporal precision. A myriad of optoswitches has been engineered and applied in prokaryotic and eukaryotic cells to regulate gene expression, subcellular protein localization, enzyme activity, and even to develop light-controllable biohybrid materials among other processes and systems (see www.optobase.com).[1]

The late explosion of enabling technologies to modulate the flow of genetic information, made possible through methods that derive from clustered regularly interspaced short palindromic repeats (CRISPR)-based techniques, currently positively reshapes biological studies.[2] Key applications of the specific DNA-recognizing CRISPR/Cas9 systems encompass for example genome editing and transcriptional regulation with high sequence specificity.[2–6] In recent years, these technologies led to major advances in synthetic biology, gene therapy, and gene modification in almost every model organism. Various Cas-variants were subsequently derived from different microorganisms and utilized to overcome some of the limitations restricting in vivo applications, or enabled the recognition of RNA instead of DNA.[2,7–9] Among those, the discovery of the RNA-targeting Cas13 proteins yielded in powerful RNA-editing tools.[9,10] Cas13 belongs to type VI CRISPR effectors and has been utilized for specific knockdown of endogenous RNAs in human cells and manipulation of alternative RNA splicing.[9,11] While the DNA-targeting CRISPR/Cas9 systems require the presence of a short protospacer adjacent motif (PAM) sequence at the editing site, Cas13 is PAM-independent.[9,10]

Recent engineering efforts of CRISPR/Cas tools for optogenetic regulation expanded their capabilities including high spatial and temporal control precision,[12–19] however, these systems exclusively target DNA. Only few light-regulated RNA modification tools currently exist, mostly based on RNA interference or short regulatory RNAs, which are CRISPR-independent.[20–23]

We devised here an optogenetic tool to destabilize cellular mRNA by enabling optical control of RNA-targeting CRISPR/Cas13 systems. For this, we combined a blue light-inducible gene expression switch[24] with the *Prevotella sp.*-derived Cas13 effector (*Psp*Cas13b),[9] resulting in a system termed Lockdown (blue light-operated CRISPR/Cas13b-mediated mRNA knockdown). Blue light activates the gene switch to induce the expression of *Psp*Cas13b which, in the presence of a gRNA targeting the mRNA of interest, leads to downregulation of said RNA. Our results demonstrate how Lockdown can be used to regulate cellular processes with blue light through specific mRNA degradation. In our tests, these induced G2 cell cycle arrest and inhibition of cell growth under blue light.[25,26] We further combined Lockdown with the recently published "Blue-OFF" system for synergistic triple-targeted downregulation of proteins.[27,28]

To engineer the Lockdown system, we used a split transcription factor based on a modified light-oxygen-voltage domain

T. Blomeier, Dr. P. Fischbach, L.-A. Koch, Dr. J. Andres,
Dr. M. Miñambres, Dr. H. M. Beyer, Prof. M. D. Zurbriggen
Institute of Synthetic Biology and CEPLAS
University of Düsseldorf
Düsseldorf 40225, Germany
E-mail: matias.zurbriggen@uni-duesseldorf.de
Dr. M. Miñambres
Institute of Plant Biochemistry and CEPLAS
University of Düsseldorf
Düsseldorf 40225, Germany

**ADVANCED
SCIENCE NEWS**

www.advancedsciencenews.com
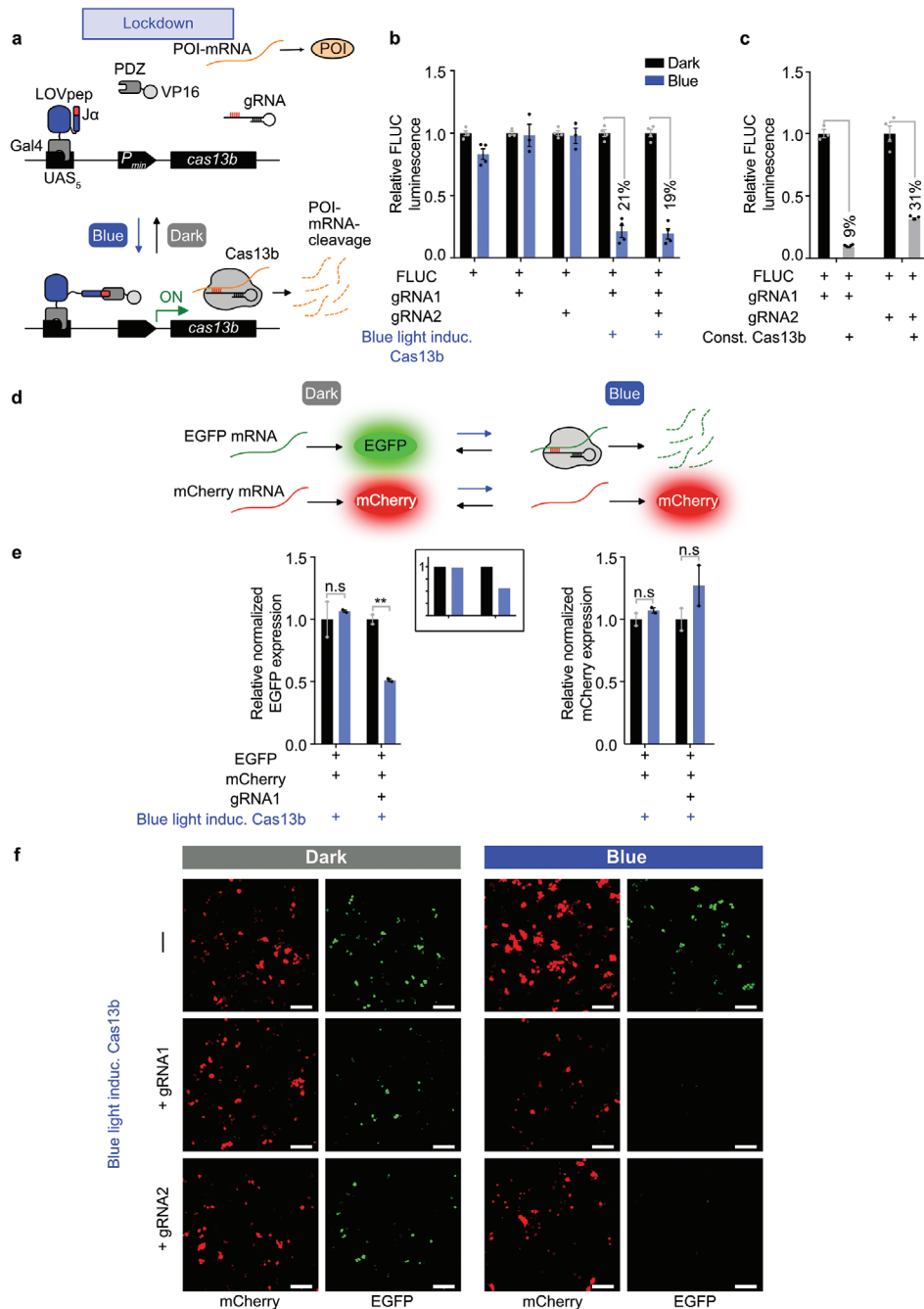
**ADVANCED
BIOLOGY**

www.advanced-bio.com

Figure 1. Design and characterization of the Lockdown system. a) Lockdown architecture. The blue light-responsive split transcription factor, bound to DNA via Gal4, activates expression of the gene encoding Cas13b upon illumination. Light recruits the transcriptional activator VP16 via exposure of a PDZ-interacting epitope embedded in the Jα helix. A specific gRNA guides Cas13b to cleave a target mRNA encoding a protein of interest (POI). b) Co-expression of FLUC-specific gRNA1 (pTBPF003) or gRNA2 (pTBPF004) causes reduction of FLUC (pTBPF015) levels in HEK-293T cells using Lockdown to control the expression of Cas13b. The cells were either illuminated with 460 nm light for 24 h (blue bars) or kept in the dark (black bars). Values from illuminated samples were normalized to the corresponding sample kept in the dark. c) Experiment as in (b), but with co-expression of constitutive Cas13b (pC0046). Data were normalized to the conditions lacking the Cas13b expression plasmid. (b,c) $n = 4$; error bars represent one standard error of the mean (SEM). d) Schematic of the blue light-induced knockdown of EGFP mRNA. Under blue light, Lockdown specifically degrades mRNA encoding EGFP while leaving mCherry unaffected. e) Quantification of EGFP (left) and mCherry (right) expression via qRT-PCR. HEK-293T cells were co-transfected with the blue light switch, P$_{PGK}$-EGFP, and P$_{SV40}$-mCherry. An EGFP-specific gRNA was included (gRNA1, pTBPF005). Illumination for 48 h was started 4 h post transfection, or cells were kept in the dark. $n = 2$; error bars represent one standard error of the mean (SEM). Significance was calculated with a paired students t-test (*$P < 0.05$; **$P < 0.01$; ***$P < 0001$). Inlet figure (center) shows the quantification of normalized intensities of an α-EGFP western blot analysis of the same experiment (see Figure S5, Supporting Information). f) Microscopic analysis of EGFP and mCherry expression. HEK-293T cells were co-transfected with Lockdown and EGFP-specific gRNAs (-, none; gRNA1, pTBPF005; gRNA2, pTBPF006). Illumination conditions as in (e). Pictures were acquired by confocal imaging of EGFP and mCherry. Scale bar, 100 µm.

**ADVANCED
SCIENCE NEWS**

www.advancedsciencenews.com

**ADVANCED
BIOLOGY**

www.advanced-bio.com

from phototropin 1 of *Avena sativa* (*As*LOV2) to express an engineered variant of *Psp*Cas13b (**Figure 1**a).[9,24,29] We placed the gene encoding *Psp*Cas13b downstream of a minimal human cytomegalovirus promoter harboring five adjacent repeats of the Gal4 upstream activating sequence (UAS$_5$). Bound to DNA via fusion to the Gal4 DNA-binding domain, *As*LOV2 exposes a C-terminal epitope tag through relaxation of the Jα-helix under blue light. Tag exposure recruits the transcriptional activation domain VP16, which is fused to the tag-interacting ePDZ domain and leads to initiation of *Psp*Cas13b gene transcription and subsequent translation. Constitutive co-expression of a sequence-specific gRNA in *trans*, guides *Psp*Cas13b to cleave target RNAs. Due to the half life time of the *As*LOV2 domain in the excited state of 17 s,[29] the transcriptional activation complex rapidly dissociates in the darkness stopping further transcription of *Psp*Cas13b.[24]

We first tested whether Lockdown would specifically downregulate mRNA under blue light (Figure 1b,c). We designed two gRNAs targeting Firefly luciferase (FLUC) mRNA and co-expressed them with FLUC in Human embryonic kidney cells (HEK-293T). As expected, only the presence of a suitable gRNA and blue light illumination (10 µmol m^{-2} s^{-1} at 460 nm for 24 h) reduced FLUC-levels down to about 20% compared to levels obtained from cells kept in the dark (Figure 1b). The repression levels under blue light matched the levels obtained upon constitutive *Psp*Cas13b expression (Figure 1c).[9]

In order to assess the functionality of the system in a different experimental setup, and in particular for future mid-throughput applications, we illuminated Chinese hamster ovary cells (CHO-K1) in 96-well glass bottom plates with different blue light intensities using an optoPlate-96 illumination device (Figure S1, Supporting Information).[30,31] In this multi-well plate format, the downregulation of FLUC levels under blue light compared well with the results in HEK-293T cells (Figure 1b), even at lower light intensities.

We next set to complete the evaluation of the functionality of the system, by performing an experiment to analyze the effects of Lockdown as reflected at the mRNA and protein levels using three different methods (Figure 1d–f). For this, we designed two EGFP-specific gRNAs and expressed EGFP from a constitutive PGK promoter. Co-expression of mCherry served as control to validate that loss of EGFP abundance under blue light occurs specifically and not as a result of an artifact. Quantitative real-time PCR (qRT-PCR) experiments showed a clear reduction in mRNA levels for EGFP while those of mCherry remained comparable between samples that where either illuminated with blue light or kept in the dark (Figure 1e). The mRNA degradation effects also showed the expected dependence on the presence of a corresponding selective gRNA. In a microscopic analysis at the whole cell level, EGFP fluorescence remained unaffected in the absence of the Lockdown components with the matching gRNA, regardless of the illumination condition (Figure 1f, upper panel and Figure S2, Supporting Information). In contrast, the Lockdown system including either gRNA strongly reduced the EGFP signal in blue light conditions, while mCherry remained comparable in all conditions (Figure 1f, lower panels and Figure S2, Supporting Information). We further confirmed the microscopically-observed reduction in EGFP

signal under blue light using western blot analysis (Figure 1e (center) and Figure S5, Supporting Information).

Methods for downregulation of protein abundance usually target only one step of the gene expression process, which spans from the regulation of transcriptional initiation of a specific gene up to ribosomal translation into the final protein and the stability thereof.[7,32] However, these methods are often insufficient to entirely block and/or reduce the abundance of a specific protein. A recently published optogenetic system for downregulation of protein levels (Blue-OFF) demonstrated the effect of a synergistic regulation on different levels.[27] The system consists of two components, B-LID (blue light-inducible degradation domain), a blue light-activated protein degradation module fused to the protein of interest, and the light-responsive KRAB-EL222 repressor protein. Combined light-induced repression of transcription using KRAB-EL222 and protein stability with B-LID decreased the abundance of given cellular target proteins substantially.[27] The remaining protein levels present after induction of transcriptional repression and protein degradation likely result from mRNA transcribed before the repression was exerted. Hence, we hypothesize that by degrading the remaining mRNA, Lockdown could contribute to a quantitative loss of the protein. We therefore combined the Blue-OFF system with Lockdown to simultaneously repress the abundance of FLUC on three regulation levels: transcriptional repression, mRNA degradation, and protein degradation (**Figure 2**a,b). First, we transfected HEK-293T cells with the different components of the Blue-OFF system achieving a reduction of the relative protein abundance down to 3,3% after induction with blue light in comparison to darkness (Figure 2b and Figure S3, Supporting Information). The combination of Lockdown utilizing any of the gRNAs (see Figure 1b,c) with the Blue-OFF system led to a reduction of around 99% of FLUC under blue light, demonstrating the advantages of integrating the different systems for the quantitative depletion of a protein of interest.

To demonstrate the ability of Lockdown to regulate cellular processes, we aimed at knocking down endogenous genes in mammalian cells. Since this approach does not require further protein engineering, one can in principle easily adapt the strategy to any endogenous RNA by expressing an ad hoc designed gRNA. The human cyclin-dependent kinase 1 (Cdk1)-family of kinases constitutes one of the main regulators integrating external and internal stimuli that influence cell cycle control and cell division.[25,33–36] Cdk1 plays an essential role at the checkpoint coordinating the G2/M phase transition.[25,26,37,38] Inhibition of Cdk1 in human cells stalls the cell cycle through a G2/M arrest, and dysregulation of factors associated with the control of Cdks frequently engage in tumor development.[34] We designed two gRNAs targeting endogenously produced human CDK1 mRNA and tested the effects caused by blue light-induced degradation in HEK-293T cells (**Figure 3**a,b). Lockdown including either of the gRNA led to a significant reduction in the total cell count when cells were illuminated with blue light (Figure 3b and Figure S4, Supporting Information). The observations demonstrate the feasibility of a generalized use and the applicability of Lockdown for the blue light-dependent downregulation of endogenous mRNAs.

Use of RNA interference approaches and riboswitches have significantly contributed to groundbreaking advances in life
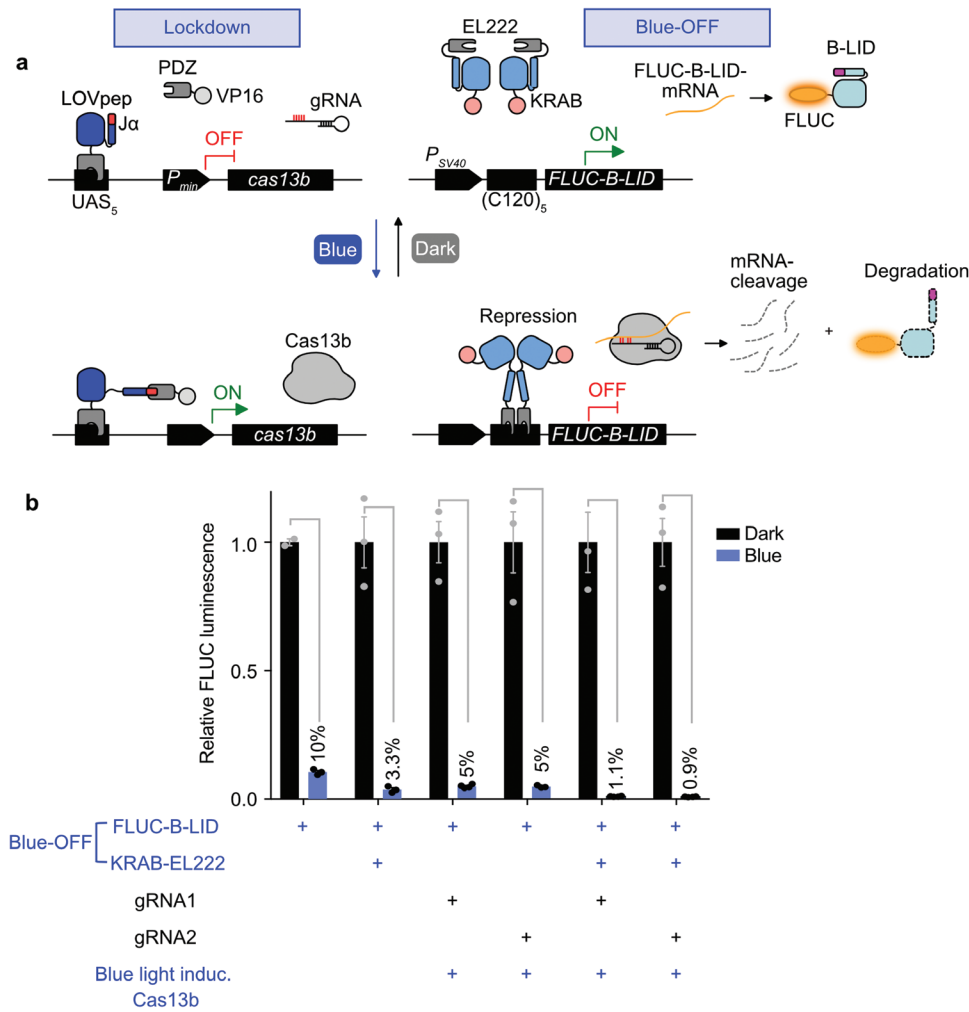
**ADVANCED
SCIENCE NEWS**

www.advancedsciencenews.com

**ADVANCED
BIOLOGY**

www.advanced-bio.com

Figure 2. Combined repression of protein levels using Lockdown and Blue-OFF. a) Schematic description of the Lockdown and Blue-OFF combination setup. In the dark, Lockdown and Blue-OFF are inactive, leading to usual expression levels of target proteins (FLUC). Under blue light, Cas13b (Lockdown) cleaves the target mRNA, whereas the KRAB-EL222 repressor protein and the B-LID degron (Blue-OFF) repress FLUC production on the transcriptional and post-translational level, respectively. Under blue light, the Blue-OFF system acts by recruiting the KRAB repressor to the promoter by binding of EL222 to 5 repeats of the C120 sequence. B-LID is fused to the FLUC target protein and exposes a RRRG-degron sequence upon illumination, leading to proteasomal degradation. b) Combinatorial analysis of the Lockdown and Blue-OFF components shown in (a). FLUC bioluminescence was determined from lysates of HEK-293T cells expressing the indicated components. The gRNAs from Figure 1b,c were used. Cells were illuminated with 460 nm light for 24 h, or kept in the dark. Values were normalized to the corresponding dark sample. $n = 4$, error bars indicate one standard error of the mean (SEM).

sciences.[39–42] These RNA tools have for example successfully been used to study signaling pathways, cancer therapeutics, and cell cycle regulation.[42,43] However, only a few optogenetic tools for the control of mRNA exist.[20–23] The here-described Lockdown system combines optogenetic regulation of transcription with RNA-guided RNA processing by the *Psp*Cas13b ribonucleoprotein to generate optogenetic control of RNA degradation. Lockdown is compatible and synergistically active with the Blue-OFF system, achieving nearly complete depletion of a protein through combined blue light-triple-induction of transcriptional repression, and mRNA and protein degradation.[27] Lockdown synergistically combines recent independent developments in synthetic biology: One is the optogenetic switch that controls the temporal and spatial resolution of the system as well as *Psp*Cas13b levels depending on blue light intensity.[24,29]

The other development is *Psp*Cas13b, which mainly contributes to the knockdown specificity of the system what indirectly influences also the overall efficacy. The *Psp*Cas13b component itself combined with Lockdown remains unchanged from earlier reports and therefore one can assume that previous characterizations of the system indicating a high specificity are valid.[9] The LOV2-based blue light photoswitch has short dark reversion kinetics, therefore the use as gene-expression system requires a near constant illumination over the desired induction time and high light intensities when used in deep tissues due to the low penetration depth of said short wavelengths. However, it benefits from the readily bioavailable FMN cofactor in contrast to red and green optogenetic switches.

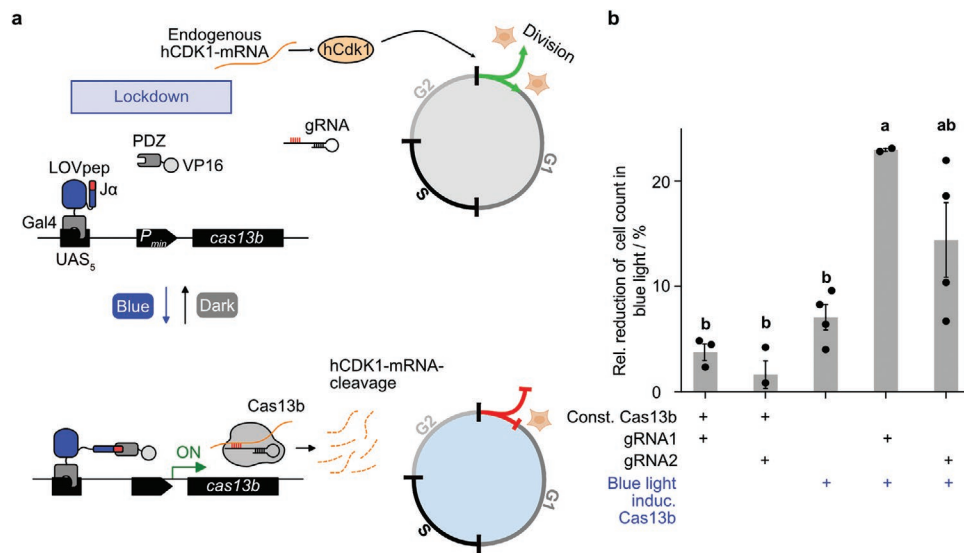The last decade has witnessed hundreds of applications where optoswitches targeted diverse cellular processes.[1] This

**ADVANCED
SCIENCE NEWS**
www.advancedsciencenews.com

**ADVANCED
BIOLOGY**
www.advanced-bio.com

Figure 3. Cell cycle control using Lockdown. a) Human Cdk1 controls cell cycle G2/M transition. Blue light illumination activates Lockdown (see Figure 1a) to degrade endogenous hCdk1 mRNA, leading to G2 cell cycle arrest and inhibition of cell division. Constitutively expressed gRNA determines the specificity for the hCdk1 mRNA. b) The total cell count was determined from HEK-293T cells expressing the indicated components. The cell count reduction in response to 24 h of blue light illumination is shown. Illumination was started 4 h post transfection. For total cell numbers see Figure S4, Supporting Information. gRNA1 and gRNA2 were expressed from plasmids pTBPF021 and pTBPF020, respectively. $n = 4$, error bars indicate one standard error of the mean (SEM). The statistical significance was determined using a one-way ANOVA analysis ($P < 0.01$) and is indicated with bold letters.

work illustrates the potential of combining optogenetic tools for the simultaneous and orthogonal control of molecular processes. We show the wide applicability by precisely targeting different exo- and endogenous mRNAs, what solely requires the ad hoc design of a specific Cas13 gRNA. Lockdown advances the precise study of physiological effects, such as modulation of the cell cycle, and holds the future potential to assist in the investigation of unknown cellular processes.

Experimental Section

All used and designed plasmids and oligonucleotides are described in Tables S1 and S2, Supporting Information. Oligonucleotides used for quantitative real-time PCR are described in Table S3, Supporting Information. All gRNAs used in this study were designed as described elsewhere and inserted into an U6 promoter-driven mammalian expression vector.[9] All gRNA sequences are described in Table S4 (Supporting Information). All experiments are based on transient plasmid transfection of the respective mammalian cells.

Human embryonic kidney cells (HEK-293T; DSMZ, Braunschweig, Germany) and Chinese hamster ovary cells (CHO-K1; DSMZ) were cultivated and seeded as described elsewhere.[44] Cells were transfected in 24-well (5×10^4 cells) or 96-well (8×10^3 cells) plates using polyethylenimine (PEI; Polysciences Inc. Europe, Hirschberg, Germany; no. 23966-1) as described.[44] If not indicated otherwise, all plasmids were transfected with the Lockdown system consisting of the *As*LOV2-based blue light system (plasmid pKM516),[24] the inducible *Psp*Cas13b (pTBPF001), and a sequence-specific gRNA plasmid (Table S4, Supporting Information) in equal amounts w/w. 24 h post transfection, cells were illuminated with 460 nm light for the indicated periods of time with a light intensity of 10 µmol m^{-2} s^{-1} or kept in darkness (typically for 24 h, unless indicated otherwise). Samples were illuminated using custom built LED light boxes housing 460 nm light-emitting LEDs.[45] In Figure S1, Supporting Information, illumination was done in

optoPlate-96 illumination devices.[30,31] Cell culture work was performed using safe light (522 nm) to prevent unintended activation of the light-sensitive systems.

To quantify luciferase bioluminescence, cells were lysed and incubated as previously described.[27] For cells grown in 96-well plates, the supernatant was removed and the substrate was directly added to the cells without prior cell lysis. Luminescence was monitored using a Centro XS^3 LB960 Microplate Luminometer (Berthold Technologies, Bad Wildbad, Germany). Confocal imaging was performed with an Eclipse Ti microscope (Nikon, Tokyo, Japan) equipped with a C2plus confocal laser scanner and a 20x air objective, NA = 0.45. Cells were seeded on glass coverslips and fixed with paraformaldehyde as described.[46] EGFP and mCherry fluorescence were visualized using an excitation laser of 488 and 561 nm and emission filters of 505–545 and 570–620 nm, respectively.

For qRT-PCR experiments, RNA was isolated using the NucleoSpin RNA Plus Kit (Macherey Nagel, Düren, Germany). The yielded RNA was further converted into cDNA utilizing the LunaScript RT SuperMix Kit (NEB, Ipswich, MA, USA). qRT-PCR experiments were conducted using a OneStepPlus Real-Time PCR system Thermal Cycling Block (Applied Biosystems, Foster City, CA, USA) and a Luna Universal Probe qPCR Master Mix (NEB) with 10 ng of cDNA per sample in triplicate reactions. Cycling conditions were set according to the master mix manufacturer's protocol.

For western blot experiments, HEK-293T cells were lysed in radioimmunoprecipitation buffer (150×10^{-3} M NaCl, 20×10^{-3} M Tris-HCl, pH 7.5, 0.1% NP40, 5×10^{-3} M EDTA) containing cOmplete Mini protease inhibitor (Roche, Basel, Switzerland). The lysates were centrifuged at 13 000 g for 10 min at 4 °C and the supernatants were transferred into new reaction tubes. The samples were mixed with 4x SDS buffer (Sigma Aldrich, St. Louis, MO, USA) (4:1) and incubated at 95 °C for 10 min. 10 µL of each sample were separated by SDS-PAGE on a 15% polyacrylamide gel and subsequently transferred onto a polyvinylidene fluoride membrane (Bio-Rad Laboratories, Hercules, CA, USA). The membranes were treated with the anti-GFP (Torrey Pines Biolabs, Secaucus, NJ, USA; TP-401) or anti-Actin (Sigma-Aldrich; A2066) primary antibodies. Protein detection was performed using an

anti-rabbit secondary antibody conjugated to horseradish peroxidase (Cell Signaling, Danvers, MA, USA; 7074S) and the ECL detection kit (GE Healthcare, Chicago, IL, USA). Chemiluminescence was visualized using a Universal Hood III imaging system (Bio-Rad Laboratories). Band intensities were measured using ImageJ (National Institutes of Health, Bethesda, MD, USA) and normalized to the respective loading control.

For cell proliferation assays, HEK-293T cells (30×10^4 cells) were seeded in 24-well cell culture dishes and transfected as described above. Illumination was started 4 h post transfection as described before. The next day, cells were trypsinized (250 µL, Trypsin/EDTA, PAN Biotech, Aidenbach, Germany; P10-023500) for 4 min at 37 °C and resuspended. DMEM complete medium (1 mL) was added and cell suspension (200 µL) was added to CASYton buffer (10 mL, OMNI Life Science, Bremen, Germany; 5 651 808) inside a CASYcup (OMNI Life Science) before the cell concentration was determined by electronic current exclusion (ECE) technology with a Cell counter CASY (OMNI Life Science).

Data analysis, calculation of corresponding *P*-values, and generation of graphs were done using GraphPad Prism 7 (GraphPad Software, Inc.). Data from illuminated samples shown in Figures 1b,e and 2b and Figures S1, S3 and S4 (Supporting Information) were normalized to the corresponding sample kept in the dark. In Figure 1c, data were normalized to the conditions lacking the Cas13b expression plasmid. Significance of equally treated samples of the respective light conditions in Figure 1e was calculated using a paired two-sided student's *t*-test. The statistical significance of reduction in total cell numbers in Figure 3b was determined using a one-way ANOVA analysis ($P < 0.01$) and is indicated with bold letters. Statistical outliers were determined and excluded as described elsewhere.[47]

Supporting Information

Supporting Information is available from the Wiley Online Library or from the author.

Conflict of Interest

The authors declare no conflict of interest.

Data Availability Statement

Data and materials are available on request.

[1] K. Kolar, C. Knobloch, H. Stork, M. Žnidarič, W. Weber, *ACS Synth. Biol.* **2018**, *7*, 1825.

[2] A. Pickar-Oliver, C. A. Gersbach, *Nat. Rev. Mol. Cell Biol.* **2019**, *20*, 490.

[3] M. Tabebordbar, K. Zhu, J. K. W. Cheng, W. L. Chew, J. J. Widrick, W. X. Yan, C. Maesner, E. Y. Wu, R. Xiao, F. A. Ran, L. Cong, F. Zhang, L. H. Vandenberghe, G. M. Church, A. J. Wagers, *Science* **2016**, *351*, 407.

[4] D. G. Ousterout, A. M. Kabadi, P. I. Thakore, W. H. Majoros, T. E. Reddy, C. A. Gersbach, *Nat. Commun.* **2015**, *6*, 6244.

[5] P. D. Hsu, E. S. Lander, F. Zhang, *Cell* **2014**, *157*, 1262.

[6] A. V. Anzalone, P. B. Randolph, J. R. Davis, A. A. Sousa, L. W. Koblan, J. M. Levy, P. J. Chen, C. Wilson, G. A. Newby, A. Raguram, D. R. Liu, *Nature* **2019**, *576*, 149.

[7] C. Fellmann, B. G. Gowen, P.-C. Lin, J. A. Doudna, J. E. Corn, *Nat. Rev. Drug Discovery* **2017**, *16*, 89.

[8] S. C. Strutt, R. M. Torrez, E. Kaya, O. A. Negrete, J. A. Doudna, *Elife* **2018**, *7*, 32724.

[9] D. B. T. Cox, J. S. Gootenberg, O. O. Abudayyeh, B. Franklin, M. J. Kellner, J. Joung, F. Zhang, *Science* **2017**, *358*, 1019.

[10] A. K. Brooks, T. Gaj, *Curr. Opin. Biotechnol.* **2018**, *52*, 95.

[11] S. Konermann, P. Lotfy, N. J. Brideau, J. Oki, M. N. Shokhirev, P. D. Hsu, *Cell* **2018**, *173*, 665.

[12] L. R. Polstein, C. A. Gersbach, *Nat. Chem. Biol.* **2015**, *11*, 198.

[13] Y. Nihongaki, F. Kawano, T. Nakajima, M. Sato, *Nat. Biotechnol.* **2015**, *33*, 755.

[14] F. Bubeck, M. D. Hoffmann, Z. Harteveld, S. Aschenbrenner, A. Bietz, M. C. Waldhauer, K. Börner, J. Fakhiri, C. Schmelas, L. Dietz, D. Grimm, B. E. Correia, R. Eils, D. Niopek, *Nat. Methods* **2018**, *15*, 924.

[15] Y. Nihongaki, Y. Furuhata, T. Otabe, S. Hasegawa, K. Yoshimoto, M. Sato, *Nat. Methods* **2017**, *14*, 963.

[16] Y. Yu, X. Wu, N. Guan, J. Shao, H. Li, Y. Chen, Y. Ping, D. Li, H. Ye, *Sci. Adv.* **2020**, *6*, eabb1777.

[17] X. X. Zhou, X. Zou, H. K. Chung, Y. Gao, Y. Liu, L. S. Qi, M. Z. Lin, *ACS Chem. Biol.* **2018**, *13*, 443.

[18] Y. Chen, X. Yan, Y. Ping, *ACS Mater. Lett.* **2020**, *2*, 644.

[19] X. Chen, Y. Chen, H. Xin, T. Wan, Y. Ping, *Proc. Natl. Acad. Sci. USA* **2020**, *117*, 2395.

[20] P. Vogel, A. Hanswillemenke, T. Stafforst, *ACS Synth. Biol.* **2017**, *6*, 1642.

[21] N. Y. Kim, S. Lee, J. Yu, N. Kim, S. S. Won, H. Park, W. D.o Heo, *Nat. Cell Biol.* **2020**, *22*, 341.

[22] A. M. Weber, J. Kaiser, T. Ziegler, S. Pilsl, C. Renzl, L. Sixt, G. Pietruschka, S. Moniot, A. Kakoti, M. Juraschitz, S. Schrottke, L. Lledo Bryant, C. Steegborn, R. Bittl, G. Mayer, A. Möglich, *Nat. Chem. Biol.* **2019**, *15*, 1085.

[23] S. Pilsl, C. Morgan, M. Choukeife, A. Möglich, G. Mayer, *Nat. Commun.* **2020**, *11*, 4825.

[24] K. Müller, R. Engesser, J. Timmer, M. D. Zurbriggen, W. Weber, *ACS Synth. Biol.* **2014**, *3*, 796.

[25] M. Malumbres, *Genome Biol.* **2014**, *15*, 122.

[26] R. Prevo, G. Pirovano, R. Puliyadi, K. J. Herbert, G. Rodriguez-Berriguete, A. O'Docherty, W. Greaves, W. G. McKenna, G. S. Higgins, *Cell Cycle* **2018**, *17*, 1513.

[27] J. Baaske, P. Gonschorek, R. Engesser, A. Dominguez-Monedero, K. Raute, P. Fischbach, K. Müller, E. Cachat, W. W. A. Schamel, S. Minguet, J. A. Davies, J. Timmer, W. Weber, M. D. Zurbriggen, *Sci. Rep.* **2018**, *8*, 15024.

[28] P. Fischbach, P. Gonschorek, J. Baaske, J. A. Davies, W. Weber, M. D. Zurbriggen, *Methods Mol. Biol.* **2020**, *2173*, 159.

[29] D. Strickland, Y. Lin, E. Wagner, C. M. Hope, J. Zayner, C. Antoniou, T. R. Sosnick, E. L. Weiss, M. Glotzer, *Nat. Methods* **2012**, *9*, 379.

[30] L. J. Bugaj, W. A. Lim, *Nat. Protoc.* **2019**, *14*, 2205.

[31] O. S. Thomas, M. Hörner, W. Weber, *Nat. Protoc.* **2020**, *15*, 2785.

[32] F. Crick, *Nature* **1970**, *227*, 561.

[33] A. V. Leopold, K. G. Chernov, V. V. Verkhusha, *Chem. Soc. Rev.* **2018**, *47*, 2454.

[34] M. Malumbres, A. Carnero, *Prog. Cell Cycle Res.* **2003**, *5*, 5.

[35] D. O. Morgan, *Annu. Rev. Cell Dev. Biol.* **1997**, *13*, 261.

[36] S. Lim, P. Kaldis, *Development* **2013**, *140*, 3079.

[37] M. C. de Gooijer, A. van den Top, I. Bockaj, J. H. Beijnen, T. Würdinger, O. van Tellingen, *FEBS Open Bio* **2017**, *7*, 439.

[38] M. Malumbres, M. Barbacid, *Nat. Rev. Cancer* **2009**, *9*, 153.

[39] M. Vogel, J. E. Weigand, B. Kluge, M. Grez, B. Suess, *Nucleic Acids Res.* **2018**, *46*, 48.

[40] K. J. Dery, V. Gusti, S. Gaur, J. E. Shively, Y. Yen, R. K. Gaur, *Methods Mol. Biol.* **2009**, *555*, 127.

[41] A. M. Celotto, B. R. Graveley, *RNA* **2002**, *8*, 718.

[42] C. P. Dillon, P. Sandy, A. Nencioni, S. Kissler, D. A. Rubinson, L. Van Parijs, *Annu. Rev. Physiol.* **2005**, *67*, 147.

[43] M. Sierant, D. Piotrzkowska, B. Nawrot, *Acta Neurobiol. Exp.* **2015**, *75*, 36.

[44] K. Müller, R. Engesser, S. Schulz, T. Steinberg, P. Tomakidi, C. C. Weber, R. Ulm, J. Timmer, M. D. Zurbriggen, W. Weber, *Nucleic Acids Res.* **2013**, *41*, 124.

[45] K. Müller, R. Engesser, S. Metzger, S. Schulz, M. M. Kämpf, M. Busacker, T. Steinberg, P. Tomakidi, M. Ehrbar, F. Nagy, J. Timmer, M. D. Zubriggen, W. Weber, *Nucleic Acids Res.* **2013**, *41*, 77.

[46] H. M. Beyer, S. Juillot, K. Herbst, S. L. Samodelov, K. Müller, W. W. Schamel, W. Römer, E. Schäfer, F. Nagy, U. Strähle, W. Weber, M. D. Zurbriggen, *ACS Synth. Biol.* **2015**, *4*, 951.

[47] J. L. Jacobs, J. D. Dinman, *Nucleic Acids Res.* **2004**, *32*, 160.